Ocean Sci. Discuss., 12, 735–767, 2015
www.ocean-sci-discuss.net/12/735/2015/
doi:10.5194/osd-12-735-2015


Ocean Science
Discussions
Open Access



# Interactions between the Somali Current eddies during the summer monsoon: insights from a numerical study

**C. Q. C. Akuetevi[1,2], B. Barnier[2], J. Verron[2], J.-M. Molines[2], and A. Lecointre[3]**

[1]Université Grenoble Alpes, LEGI, CNRS, 38000 Grenoble, France
[2]Université Grenoble Alpes, LGGE, CNRS, 38000 Grenoble, France
[3]Université Grenoble Alpes, ISTerre, CNRS, 38041 Grenoble,France

Received: 30 March 2015 – Accepted: 23 April 2015 – Published: 19 May 2015

Correspondence to: C. Q. C. Akuetevi (cyrille.akuetevi@legi.grenoble-inp.fr)

Published by Copernicus Publications on behalf of the European Geosciences Union.

## Abstract

Three hindcast simulations of the global ocean circulation differing by resolution (1/4 or 1/12°) or parameterization or atmospheric forcing are used to study the fast interactions between the large anticyclonic eddies generated by the Somali Current system during the Southwest Monsoon. The present investigation of the Somalian coherent eddy structures allows us to identify the origin and the subsequent development of the cyclones flanked upon the Great Whirl (GW) previously identified by Beal and Donohue (2013) in satellite observations and to establish that similar cyclones are also flanked upon the Southern Gyre (SG). These cyclones are identified as major actors in mixing water masses within the large eddies and offshore the coast of Somali.

All three simulations bring to light that during the period when the Southwest Monsoon is well established, the SG moves northward along the Somali coast and encounter the GW. The interaction between the SG and the GW is a collision without merging, collision during which the GW is pushed to the east of Socotra Island, sheds several smaller patches of anticyclonic vorticity, and often reforms into the Socotra Eddy, thus proposing a formation mechanism for the Socotra Eddy. During this process, the GW gives up its place to the SG which in turn becomes a new Great Whirl. This process is robust throughout the three simulations.

## 1 Introduction

The near-surface circulation of the northwestern Indian Ocean during the summer monsoon is the siege of large and strong anticyclonic eddies produced by recirculation cells of the Somali current system. In the schematic representation of the typical surface current patterns proposed in the comprehensive review of Schott and McCreary (2001) and updated in Schott et al. (2009, their Fig. 3, see also our Fig. 1), the *South Equatorial Current* (SEC) and the *East African Coastal Current* (EACC) are supplying the *Somali Current* (SC), a low-latitude western boundary current flowing northward along





OSD

12, 735–767, 2015

Somali Current eddies interactions

C. Q. C. Akuetevi et al.

the coast of Somali at this time of the year. A large branch of the EACC turns offshore after crossing the equator at about 2 or 3° N and forms the so-called *Southern Gyre* (SG), a large anticyclonic retroflection cell with a well marked wedge of cold upwelled water attached to its northern flank (the *southern cold wedge*). According to Beal et al. (2013), this cell re-circulates southward across the equator to feed into the *South Equatorial Counter Current* (SECC). In the North, located between the SG and the island of Socotra (i.e. between 5 and 10° N) is the *Great Whirl* (GW), a large anticyclone which exhibits very intense swirling currents. The GW also exhibits an upwelling wedge at its northern flank (the *northern cold wedge*). A third anticyclonic eddy named the *Socotra Eddy* (SE) is reported to be frequently present to the northeast of the Island of Socotra.

It has been very difficult to follow the time evolution of these large eddies from direct observations due to their fast development until satellite altimeter measurements could provide a dense enough mapping of the sea surface height (SSH). The analysis of 18 years of weekly AVISO SSH fields by Beal and Donohue (2013) revealed a fast and chaotic evolution of the GW, variations is size, shape and location of the eddy being greatly influenced by strong eddy–eddy interactions. Such behavior was suggested by the idealized numerical model studies of Jensen (1991) or Wirth et al. (2002). This contrasts with the previous studies which convey the view of a GW that is slowly varying in response to the wind forcing (e.g. Schott and McCreary, 2001). Beal and Donohue (2013) observed that one to three cyclonic eddies of smaller size are flanking the GW most of the time, appearing in late June and circulating clockwise around the GW. They also observed the Socotra Eddy, but found that its variability in shape, size and position was even greater than the one seen for the GW, making the SE often difficult to identify. Nevertheless, they report its frequent merging with the GW. At the best of our knowledge there is still no clear formation mechanism proposed for this eddy. The analysis of Beal and Donohue (2013) does not report any interaction between the Southern Gyre and the GW, possibly because they limited the domain of study to 3–15° N. However, the northward migration of the SG and its possible merging with the GW is mentioned in several observational studies (Evans and Brown, 1981; Swallow et al., 1983).





OSD
12, 735–767, 2015

Based on the observation of a merging of the southern cold wedge with the northern one, those studies suggest that the SG and the GW could coalesce. Such merging was also observed in the numerical model study of Luther and O'Brien (1989), but was not reported in the observations collected during the WOCE cruises of 1995–1996 (Schott et al., 1997).

The lack of understanding that remains regarding the processes that govern the dynamics of the large circulation features or large coherent structures that are the Southern Gyre, the Great Whirl and the Socotra Eddy, largely resides in the lack of dense in space and time observations. The objective of the present study is to gain insights into the nature of the interactions between these anticyclonic eddies. The paper addresses the following questions:

- What is the generating mechanism of the cyclones flanking the Great Whirl?
- What is the nature of the interactions between the Southern Gyre and the Great Whirl, and does the merging of the southern and northern cold wedges necessarily implies a coalescence of the two eddies?
- What is the formation mechanism of the Socotra Eddy?

In regard to the lack of dense in space and time observations that entangles our understanding of the fast dynamics of the Somali Eddies, we address the above questions through realistic numerical eddying model simulations, since they can provide dense spatiotemporal information required for a synoptic description of the mesoscale circulation.

The numerical model experiments that are the basis of our analysis are described in Sect. 2. The ability of the model to reproduce the upper layer circulation in the Arabian Sea during the summer Monsoon is assessed in Sect. 3. Section 4 performs a description and an analysis of the fast dynamics of the Somali Current Eddies as simulated by the model experiments. Section 5 discusses the results put forward by our analysis, of the eddy–eddy interactions in the western Arabian Sea and summarizes the main findings.





OSD
12, 735–767, 2015

## 2 Numerical model simulations

Three global ocean hindcast simulations, one at $1/4^\circ$ resolution and two at $1/12^\circ$ resolution, made available by the DRAKKAR consortium (DRAKKAR-Group et al., 2007, 2014), are used here to study the Somali eddies during the southwest monsoon.

The model configurations used to produce these hindcasts are based on the NEMO ocean/sea-ice general circulation numerical model (Madec, 2008) and utilize specifications developed by the DRAKKAR consortium. Among them is the ORCA025 eddy-permitting configuration which has a nominal resolution at the equator of 0.25° and 75 vertical levels. ORCA025 is extensively described in Barnier et al. (2006) and has been widely used to address scientific questions in physical oceanography, biogeochemistry, and marine biology (see refereed publications at www.drakkar-ocean.eu). The other is the ORCA12 eddy-resolving configuration with a resolution of $1/12^\circ$ and 46 vertical levels. ORCA12 is the most recent and the highest resolution global configuration of the DRAKKAR hierarchy, and its effective horizontal resolution ranges between 9.25 km at the Equator, 7 km at Cape Hatteras (mid-latitudes), and 1.8 km in the Ross and Weddell Seas. Models of that resolution have been shown to drastically improve the representation of western boundary currents (Maltrud and McClean, 2005; Maze et al., 2013). Driven by atmospheric forcing derived from atmospheric reanalysis (Brodeau et al., 2010), ORCA12 simulations are good tools to investigate global dynamical and thermo-dynamical balances.

For example, ORCA12 has been used very recently to document the transport of salinity anomalies at 30° S in the Atlantic and its link with the stability of the Atlantic meridional overturning circulation (Deshayes et al., 2013). It was also used to understand the eddy driven mechanisms contributing to the salinity budget in the ocean (Treguier et al., 2014), and to quantify the influence of the variability in density around the Canary Islands on the Atlantic meridional overturning circulation (Duchez et al., 2014), to study the North Atlantic sub-polar circulation in an eddying regime (Marzocchi et al., 2015), or to characterize the spatial scales of the low-frequency intrinsic sea-level variability in the global ocean (Serazin et al., 2015).

The specificities of the three simulations used here are presented in Table 1. Main differences between the simulations lie in the horizontal resolution (1/4 or 1/12°) or vertical resolution (75 or 46 levels), in the atmospheric forcing used which can be ERA-interim (Dee et al., 2011), the DFS4.3 atmospheric forcing (Brodeau et al., 2010) or the CORE forcing (Large and Yeager, 2009), in the length of integration which can vary from 15 to 30 years, and in the side wall boundary conditions which can be free slip or partial slip. The differences between the simulations are not used to investigate the model sensitivity but to provide some assessment on the robustness of our results to some changes in model configuration, the features described in the paper being robust or not through all the three simulations. The analysis of model results presented here is performed on the last 10 years of every simulation using model outputs every 5 days.

## 3 Arabian upper-layer circulation during the summer monsoon

The ability of the above model configurations to realistically simulate the large-scale and mesoscale features of the global ocean circulation has been demonstrated in several studies (as mentioned in the previous section). We present here a short validation of the upper-layer circulation in the Arabian Sea during the Southwest Monsoon for the 1/4° resolution ORCA025 simulation. The results described in this section also hold for the two ORCA12 simulations (except for the appearance of structures of smaller scale and some spatial and temporal lags expected from the turbulent nature of the flow), and are generally very consistent with the circulation schemes proposed in the literature (e.g. Schott et al., 2009; Beal et al., 2013).

The surface circulation in the early phase of the summer monsoon is shown in Fig. 1 a which displays the monthly mean for the month of June of the sea surface elevation and the currents at 100 m depth. From 10° S to 2° N, the EACC is well established as a northward continuous coastal current that crosses the equator. A large part of the





OSD
12, 735–767, 2015

current turns offshore at around 2° N to form the Southern Gyre, a retroflection loop that crosses back the equator and joins the eastward flow of the South Equatorial Counter-Current (SECC) at about 4° S. Part of the EACC continues flowing northward along the coast and joins the SC at 3° N. The SC flows along the coast of Somali up to 10–12° N where it loops offshore to join an intense Great Whirl easily identified in Fig. 1 a by the strong SSH high off the Horn of Africa at 6–11° N. The SC continues to flow northward beyond the GW, a branch passing through the Socotra Passage as described in Fischer et al. (1996) and Fratantoni et al. (2006), and another branch flowing around the Socotra Island by the East as reported in Schott and McCreary (2001) and in Beal et al. (2013). Both branches join again north of the Island to cross the mouth of the Gulf of Aden and flow north along the Omani coast.

In the late phase of the southwest Monsoon (month of September, Fig. 1b) after the northward migration of the SG, the EACC is fully connected with the SC to the point that it is not possible to distinguish between each current. The GW, identified by the SSH high off Somali, has grown considerably. A relative SSH high (anticyclonic circulation) is observed to the northeast of the GW (and east of the Socotra Island), it is the Socotra Eddy (SE) which forms at the end of July or at beginning of August. The intensity of the GW and the SE begin to decrease in September, and both eddies disappear completely in November (no figure shown).

At the scale of the whole Indian Ocean, the year-round large circulation patterns and the planetary wave dynamics (not shown, Akuetevi, 2014) simulated by the 1/4 and 1/12° models are in very good agreement with the analysis of satellite observations in the Arabian Sea presented by Beal et al. (2013).





OSD
12, 735–767, 2015

## 4 Fast eddy dynamics along the Somali coast

### 4.1 Method

In an attempt to answer the questions identified in the introduction, several quantities are diagnosed from the model 5 day outputs (Fig. 2). We compute the relative vorticity ($\zeta$, Fig. 2a) to characterize the dynamical aspect of eddies, and use the minimum sea surface temperature (SST, Fig. 2c) to detect the cold wedges. We compute the spiciness ($\Pi$, Fig. 2c) on isopycnal $\sigma_0 = 23.8$ (the depth of which varies between 50 and 100 m). Spiciness quantifies whether waters on a given isopycnal are warm and salty (i.e "spicy" with large values of $\Pi$) or cold and fresh (i.e. "minty" with low values of $\Pi$). Because this quantity is conserved on isopycnal surfaces in the absence of mixing and surface fluxes (Flament, 2002), it is used here as a tracer characterizing the water masses transported by eddies, or to assess mixing occurring along stream of a given current. It is particularly interesting here because it allows us to distinguish between the minty waters of southern hemisphere origin that characterize the Southern Gyre and the spicy waters of the North Indian Ocean that characterize the Great Whirl as illustrated in Fig. 2b. The velocity field (vectors) at the depth of 50 m is superimposed on the above quantities to visualize currents and eddies. To access the vertical structure of eddies, we compute the depths of the isopycnals comprised in the range $22 \leq \sigma_0 \leq 26.4$ along a section parallel to coast passing through the core of the large eddies (green line in Fig. 2a). These isopycnals spread over the first 250 m and capture well the vertical eddy shape. The current speed and the relative vorticity at 50 m depth along the section are superimposed. It is noteworthy to mention that the position of the SG and the GW at mid-June (Fig. 2) will be considered as a starting position to access the fast dynamics of these anticyclones in Sect. 4.3.





OSD
12, 735–767, 2015

## 4.2 Small cyclonic eddies

This sub-section focuses on the fast dynamic that goes along with the seasonal growth and evolution of the GW and the SG. It relies on the analysis of the 5 day snapshots of relative vorticity ($\zeta$) and current fields.

### 4.2.1 Bursts

During the northward migration of the SG in June and early July, detachments of positive vorticity from the WBC are observed in all three experiments (e.g. Figs. 3–5) around the SG and the GW. These detachments are the most intense phenomena in the three experiments exhibiting the strongest velocity and vorticity gradients, and a vertical structure that reaches beyond the thermocline depth (not shown). In the three experiments, the thin sheet of positive vorticity that stretches along the western boundary (at the inner side of the SC and the EACC on every plot of Fig. 3) breaks due to the action of the large anticyclones (the SG and the GW). The detached part is torn off the boundary by the anticyclone and moves away from the boundary (see Fig. 3). North of the detachment, the positive vorticity anomaly of the boundary current vanishes. These events were previously identified and called *bursts* in analogy with the bursts or ejections of vorticity patterns in the classical boundary-layer dynamics (see Robinson, 1991; Akuetevi and Wirth, 2014). Note that if the occurrence of the bursts compares well between all simulations, the ejection of the bursts off the boundary and their offshore transport are much better resolved at $1/12$ than at $1/4^{\circ}$ resolution as can be seen in Fig. 3.

### 4.2.2 Dipoles

The positive vorticity anomalies ejected from the boundary during the bursts spin cyclonically and generate coherent cyclonic eddies, the vertical extent of which can reach beyond 300 m depth (not shown). These cyclones often pair with the negative vorticity within the large anticyclones to form asymmetric dipoles (Fig. 3). We suggest that these cyclones are the model analogues of the "flanking cyclones" of the GW evidenced by Beal and Donohue (2013) in their analysis of satellite altimeter data. The behavior of the asymmetric dipole appears to be influenced by the trajectory of the small cyclonic vortex. Two different scenarios were observed in our simulations.

i. The cyclonic vortex remains attached to the large anticyclonic eddy, circles around it, returns towards the western boundary before being sucked up into the large anticyclonic eddy and both merge (as illustrated in Fig. 3 for the $1/12^{\circ}$ simulation). This process somewhat weakens the large anticyclonic eddy and contributes to its decay. The cyclonic vortices created by the GW most often follow this trajectory. This trajectory is the one proposed by the analysis of Beal and Donohue (2013). This process is responsible for the mixing of the minty water masses of the cold wedge within the core of the large Somali anticyclonic eddies as can be seen in the difference of spiciness of the same eddy at different dates in Fig. 5.

ii. The cyclonic vortex does not pair with large anticyclonic eddy and drifts in the open ocean. This process is a major driver of the offshore mixing of the upwelled-water masses detached from the cold wedges by the bursts.

The behavior of the bursts after ejection followed by the dipoles formation is a very well-marked phenomenon which clearly influences the circulation and the mixing of upwelled waters at larger scales. As can be seen in the properties of the water masses transported by the SG and the GW in Figs. 5 and 7 from the early to the late phase of the southwest Monsoon, the bursts, their transformation into cyclonic eddies and their chaotic behavior are greatly triggering the mixing of the upwelled waters within the eddies and offshore region of the Somali Coast. The dynamics of the bursts also injects positive vorticity within the large anticyclonic seasonal eddies (the SG and the GW), prompting the short timescale variability of these eddies, as observed by Beal and Donohue (2013), but also contributing to their decay.





OSD
12, 735–767, 2015

Note that if the dynamics of bursts and the development of dipoles are clear and well marked in the simulations at 1/12° (ORCA12), they are more diffused although noticeable at 1/4° resolution, suggesting that this later resolution permits the generation of the process but not its full development.

### 4.3 Large anticyclones

To unravel the dynamical interactions between the large Somali eddies we use the 5 day outputs of the 1/12° MAL84 and MAL95 experiments since we have shown that the fast eddy dynamics is better resolved than in the 1/4° experiment but what is described hereafter is generally valid for the 1/4° simulation.

#### 4.3.1 Interaction between Southern Gyre and the Great Whirl

At the beginning of June (4 June in Fig. 3 right panel), the GW spins up between 6 and 10° N while the SG still stretches across the equator. The intensification of the southwest monsoon during June (19 June in Fig. 3) amplifies the intensity of the GW (which nevertheless exhibits a short-term variability in position and shape due to the burst dynamics). Simultaneously the EACC strengthens and the SG begins a northward migration at a speed of 1 $\mathrm{m\,s^{-1}}$, migration that usually brings it in contact with the GW around mid-July (Fig. 3, 9 July). Then different scenarios can occur as shown in Figs. 5 to 7.

i. The SG stops its migration and remains at its location south of 5° N (Fig. 4). This is the scenario reported in most schematics of the circulation of the western Arabian Sea. The evolution of the two eddies is then dominated by their chaotic interactions with the cyclonic bursts until their dislocation when the Southwest Monsoon winds vanish. This occurred only in a few cases in our simulations.

ii. The SG collides with the GW (Fig. 5) but the two eddies do not merge. The GW is pushed to the northeast and its size is significantly reduced due to its inter-





OSD
12, 735–767, 2015

action with the topography of the Socotra Island. The interaction of the GW with the island is very chaotic. The GW often sheds patches of anticyclonic vorticity of smaller size that circulate around the island, sometimes passing through the Socotra Passage before entering in the Gulf of Aden. However, the core of the GW most of the time becomes a smaller but intense eddy located at the east/southeast of the Socotra Island, commonly called the Socotra Eddy (SE). The SG takes its place to become a new GW. This scenario is the most frequent and is robust through the simulations since it occurred 22 times over the 30 years covered by the 3 simulations altogether (nearly 75 % of the cases). This type of collision is discussed in detail in the following. In rare occasions, the GW is directly pushed through the Socotra Passage (Fig. 7) and becomes an anticyclonic vortex translating slowly into the Gulf of Aden. Note that the SST plots of Figs. 5 and 7 show a coalescence of the two cold wedges.

iii. At rare occasions the SG absorbs part of the GW during the collision process (Fig. 8). But this only occurred twice in the 1/12° MAL95 simulation which used a partial slip boundary condition. The robustness of this "merging scenario" regarding the model parameters is therefore not established and it must be considered with caution.

The three simulations despite their differences in grid resolution or parameterization show that the formation and the behavior of the large Somali anticyclones follow these scenarios which emphasize the chaotic dynamics of the Somali anticyclones and motivate a more detailed description of the collision process.

#### 4.3.2 Collision

This section addresses the question of the nature of the interaction between the SG and the GW. Some observations have suggested that the two eddies could at times collapse. This suggestion has been mainly based on the satellite observation of the rapid northward migration ($\sim 1\,\mathrm{m\,s^{-1}}$) of the southern cold wedge and its collapse with





OSD
12, 735–767, 2015

the northern cold wedge (Evans and Brown, 1981). But as strongly suggested by our model results, the coalescence of the two cold wedges does not necessarily mean that the SG and the GW are merging.

A sequence of 5 day average snapshots of the MAL84 experiment during the southwest Monsoon (July to September) in 1983 is shown in Fig. 5 to illustrate the most frequent scenario.

The initial condition of this sequence is described by the situation shown in Fig. 3 (right panel, period from 4 June to 9 July 1983 in MAL84) when the SG, initially located in the southern hemisphere and being well separated from the GW, rapidly migrates northward to encounter the GW at the beginning of July.

A few days later (14 July in Fig. 5), the cross-equatorial flow of the EACC extends up to 5° N where it turns offshore to form the northern edge of the SG which appears now as a closed anticyclonic circulation centered at about 3° N ($\zeta$ plot), embedding low spiciness "minty" waters ($\Pi$ plot). On its northern flank the SG shows a wedge of cold upwelled water shooting offshore at about 6° N, the southern cold wedge (SST plot). At this moment, the GW is well established. It appears as a very coherent anticyclonic eddy centered at about 7° N, squeezed between the SG to the south and the Socotra Island to the north and embedding waters of relatively high spiciness. North of it, the northern cold wedge (SST plot) stretches far offshore. The vertical section crossing the two eddies (Fig. 6 ) shows that they are separated by well marked fronts in density, velocity and relative vorticity.

10 days later (24 July in Fig. 5), the SG continued its northward migration (its center is now located at 5° N) colliding with the GW which begins to dislocate into vorticity patches of smaller size. The spiciness shows that no merging occurs since each core keeps its own spiciness characteristics.

Again 10 days later (3 August in Fig. 5) the SG is now located where the GW was before (its core is at about 7° N). Although its spiciness has increased due to entrainment and mixing of surrounding waters, it is still characterized by a core of low spiciness waters. The GW has moved to the northwest, has significantly reduced in size and is





OSD
12, 735–767, 2015

still squeezed between the SG and Socotra Island. It has lost its coherence but still has a core of waters of relatively high spiciness.

The fronts separating the two eddies (Fig. 6) have considerably increased their intensity (above $2\,\mathrm{m\,s^{-1}}$ for the velocity at 50 m depth, $4.5 \times 10^{-5}\,\mathrm{s^{-1}}$ in vorticity, and $1.5\,\mathrm{kg\,m^{-3}}$ in density). The strength of this "border" on the one hand, the stratification of the two eddies and their annuli of positive relative vorticity (that lead to a shielded relative vorticity structure) on the other hand are strong indication that the two eddies cannot merge (see Valcke and Verron, 1997). Note that the northern and southern cold wedges have merged.

Indeed, a month later (7 September in Fig. 5), the SG has continued its northward move, has expanded in size with increased spiciness and now occupies a place usually occupied by the GW. The Southern Gyre has thus become a *new Great Whirl* (nGW). The GW with a decreased spiciness and pushed to the east of the Socotra Island in the position where the SE is usually observed has become the Socotra Eddy. The fronts separating the two eddies are still very intense. Although the variations of spiciness (true also for temperature and salinity, not shown) of the SG and the GW during the interaction that yielded their transformation into a new GW and the SE are noticeable, their respective spiciness remained notably different. This is consistent with the ship survey observations by Fischer et al. (1996) and Schott et al. (1997, their Fig. 36) who observed a difference in surface salinities between the GW and the SE at the end of August and early September.

This formation process of the new GW and the SE were not previously identified and it challenges the collapse interpretation based on the collapse of the two cold wedges. The collision did not produce the coalescence between the SG and the GW. It appears clearly that in the simulations, the SE results from the collision without merging between the SG and the GW. This collision generally takes place from mid-July to mid-August, but exhibits a large interannual variability.

However, interactions between the GW with the Socotra Island during the collision process are very chaotic and do not always result in the generation of a well defined





OSD
12, 735–767, 2015

Socotra Eddy. As shown in another sequence in 1989 (Fig. 7), the GW may dislocate during the collision and break into anticyclones of much smaller size, some remaining nearby the Island and appearing as a non well formed SE of short life time, and some moving through the Socotra Channel into the Gulf of Aden. Therefore, rather than a well defined coherent eddy, the Socotra eddy should be seen as a patch of anticyclonic vorticity resulting from the interaction of the GW with the topography that is almost always present east of Socotra Island after the collision took place.

A merging scenario where the SG absorbs a large part of the GW during the collision process has been seen to occur in two occasions but in the MAL95 simulation only (Fig. 8). This simulation uses a partial slip boundary condition (others use free slip) which modifies the vorticity balance of the boundary current and is expected to have an impact on eddy/eddy and eddy/topography interactions. Indeed, the greatest differences between the MAL84 and MAL95 simulation (both at $1/12^{\circ}$) are seen in the way the GW dislocates in smaller vorticity patterns during its collision with the SG. Concerning the dynamics of the Somali Current eddies studied here, all simulations clearly favor the collision scenario (9/10 in MAL84, 8/10 in MJM95, and 7/10 in MAL95), differences being in details. The robustness of such a "merging scenario" regarding the model parameters is therefore not established and it must be considered with caution. But one cannot rule out that such merging may occur some years since we have no definite arguments to assess that one simulation is systematically better than the other.

To better understand the collision between the SG and the GW, it is useful to analyze the evolution of their vertical profiles (Fig. 6) that correspond to the case of collision without merging of the sequence of Fig. 5. The vertical profiles show that when eddy–eddy interactions begin (plot of 14 July) the frontier separating the two eddies at about $5^{\circ}$ N is characterised by a positive vorticity associated to a sharp vein of current ($0.8\,\mathrm{m\,s^{-1}}$) and a marked density front. This suggests that the cores of the two eddies are separated by a vorticity shield of opposite sign, that makes their merging very unlikely (Valcke and Verron, 1997). As the collision process develops (plot of 3 August) the frontier (which is now between $8$–$10^{\circ}$ N since both eddies have migrated northward) is considerably reinforced: the intensity of the positive vorticity barrier has been multiplied by 5, the current is extremely intense (> 2 m s$^{-1}$) and the density front has also drastically intensified, making the merging even more unlikely.

### 4.4 Socotra Eddy

The above analysis of the model simulations strongly suggests that the Socotra Eddy that is observed in late August is a residual of the Great Whirl after its collision with the Southern Gyre. However, the analysis of the model solution during the early stage of the southwest monsoon (June and July) shows that a Socotra Eddy like feature (i.e. a more or less coherent patch of anticyclonic vorticity located to the east of the Socotra Island) is often present (7 times over the 10 years in MAL84) even before the collision of the GW with the SG begins (Fig. 9). It generally appears in early July when the Great Whirl has grown to its full intensity. The generation of this "early" Socotra Eddy appears to be linked to the detachment of the cyclonic bursts and their advection around of the Great Whirl. The eddy may also appear as an anticyclonic meander of the main current that runs along the northern edge of the Great Whirl or as a coherent mesoscale eddy. When the collision of the SG and the GW develops, this early SE is always rapidly destroyed or absorbed by the GW which later forms a new SE. When the Southern Gyre does not migrate northward and that no collision between the SG and the GW occurs, the early SE can live until the end of the monsoon (September, Fig. 4). A similar circulation pattern has been previously reported in analyses of field observations (e.g. Fischer et al., 1996) and was given the name of Socotra Gyre. Consequently, our model simulations suggest that there is not a unique generation process for the eddies observed to the east of the Socotra Island, but that they result from different ways of interaction of the Great Whirl with the topography of the Socotra Island, interactions in which the collision with the Southern Gyre or the dynamics of the bursts has a key role. The water mass properties of the core of the eddy (e.g. spiciness) should be informative to identify which process has been at work in the formation of the eddy.





OSD
12, 735–767, 2015

## 5 Conclusions

Previous efforts to understand the Somali Current and the East African Coastal Current retroflection have focused primarily on the large-scale dynamics governing the seasonal establishment of the large anticyclones i.e. the Great Whirl and the Southern Gyre rather than on their fine-scale structures and their local interactions with the other coherent structures generated within the Somali current system. This is likely due to the lack of dense in space and time observations. High resolution model hindcast simulations used herein permitted to go beyond the view of only large anticyclones and identified small scale coherent structures which allows to some extent to give more light on the fast dynamics of Somali Current Eddies.

Three eddying global model simulations provided by the DRAKKAR consortium have been used, differing by their resolution (1/4 or 1/12°) or by their parameterization (e.g. free slip or partial slip boundary condition), or length ranging from 15 to 30 years, or atmospheric forcings. The analysis of the last 10 years of these simulations first demonstrated the model ability to reproduce with a fairly good realism the major circulation patterns of the circulation in the Northwest Indian Ocean during the southwest monsoon. The analysis of 5 days snapshots (over a total of 30 years for all three simulations together) that focused on the generation mechanism of the cyclones flanking the Great Whirl, on the nature of interaction between the Southern Gyre and the Great Whirl permit to follow the time evolution of the fast dynamics of the Somali eddies.

The Somali eddies described herein appear to be quite similar to eddies shed by low latitude Western Boundary Currents elsewhere in the global ocean, even though they are among the lowest latitude and most topographically constrained eddies. For example, the generation mechanism and ultimate structure of the Somali eddies have large similarities with the anticyclonic eddies formed in the western tropical Atlantic by the retroflection of the North Brazil Current (see e.g. Johns et al., 1990; Barnier et al., 2001). Although the basic formation mechanism and physical characteristics of these low-latitude eddies are similar, their interactions with the general circulation and





OSD
12, 735–767, 2015



C. Q. C. Akuetevi et al.

regional topography differ substantially. Indeed the Great Whirl is unique as it is first generated by remote Rossby Waves (see Beal et al., 2013; Akuetevi, 2014) and later amplified by the monsoon winds via an intensification and a retroflection of the Somali Current. Somewhat differently, the Southern Gyre is the fruit of pure retroflection of the East African Coastal Current, several retroflection events of that type eventually occurring during the monsoon cycle.

The main findings of this study can be summarized as follows.

- The smaller cyclones flanking the Great Whirl identified by Beal and Donohue (2013) in satellite observations are also found around the Southern Gyre. They are due to the tearing off from the boundary current of intense patches of positive vorticity called bursts that later get organized in coherent cyclones (see Akuetevi and Wirth, 2014). The cyclones often pair with the large anticyclones. In that case they circulate around to finally being sucked up into the anticyclones contributing to their decay or colliding with the boundary current where they are absorbed. They sometimes detached from the anticyclone to later collapse in the open ocean. These flanking cyclones are main drivers in the mixing that occurs offshore Somali and into the large anticyclones. They are also largely responsible for the short-time variability of the large anticyclone (as suggested Beal and Donohue, 2013) and imprint a strong chaotic character to the flow field.

- The interaction between the SG and the GW during July/August (when the southwest monsoon is well established) is most frequently a collision without merging (75 % of the cases over 30 years). The outcome is a partial dislocation of the GW which is pushed to the east of Socotra Island to form the Socotra Eddy and gives up its place to the Southern Gyre which in turn becomes a new Great Whirl. In rare cases the Great Whirl can be directly pushed through the Passage of Socotra. Fratantoni et al. (2006) associated this to a particularly intense southwest monsoon during August.





OSD
12, 735–767, 2015



C. Q. C. Akuetevi et al.

- The merging (total or partial) of the SG with the GW cannot be ruled out based on our model simulations but it could be rare. It did not appear as a robust phenomenon in our simulations as it was seen in only one of the simulations that we analyzed and not in the two others.
- The merging of the two cold wedges does not provide information regarding the nature of interaction of the GW and the SG since the wedges always merge independently of the interaction process.
- The Southern Gyre does not always migrate northward beyond 5° N. In that rare case (4 times over 30 years but seen at least once in every simulation), the Great Whirl and the Southern Gyre do not interact and the evolution of those two eddies is dominated by their interactions with the cyclonic bursts until their dislocation when the monsoon winds vanish.
- Model solutions also exhibit a strong interannual variability of the intra-seasonal fluctuations which is very likely related to the chaotic dynamics of the Somali eddies and in particular to their motion, collapse or collision. The fact that besides the external forcing the chaotic nature of the ocean dynamics contributes substantially to the interannual variability in the Southwest Arabian Sea was already proposed by numerical model studies (e.g. Wirth et al., 2002).

The description of the fast dynamics of the Somali current system presented here relies on an interpretation of three different global model hindcast simulations which are not the reality but an attempt to represent it as well as possible. The three simulations differ by the resolution, the boundary condition, the length of simulation or the atmospheric forcing. Hence the main scenarios described herein are robust to those model changes. But our results also highlighted other phenomena, like the complete disintegration of the GW into small vorticity patches or the merging of part of the GW into the SG, that are too rare or too specific to a given simulation to assess their non dependency upon the model parameters that were used in the simulations (e.g. side wall friction). It would be necessary to perform longer simulations, as well as simulations using other ocean models (e.g. other than NEMO) or a broader range of parameters (e.g. advection schemes or subgridscale parameterizations) in order to consolidate the robustness of our conclusions. The conclusions of the present study should also be challenged by future studies that may use sufficiently dense (in space and time) satellite observations (e.g. SWOT) or eddy resolving ocean reanalysis, thus giving opportunities to consolidate our findings or suggesting alternative explanations.

*Acknowledgements.* The authors were supported by French Ministère de l'Enseignement Supérieur et de la Recherche, Centre National de la Recherche Scientifique (CNRS) and Université de Grenoble-Alpes (UGA). This work is a contribution to the DRAKKAR GDRI. It was granted access to HPC resources under the allocations x2013-010727 and x2014-010727 attributed by GENCI to DRAKKAR, simulations being carried out at both the IDRIS and CINES supercomputer national facilities. Research leading to these results also benefited from some support provided by GMMC to DRAKKAR and by Centre National d'Etudes Spatiales (CNES).

## References

Akuetevi, C. Q. C.: Dynamics of turbulent western boundary currents at low latitude, a numerical study, PhD thesis, Université Joseph-Fourier-Grenoble I, available at: http://lgge.osug.fr/meom/Publications/pdf/these_akuetevi.pdf, 2014.

Akuetevi, C. Q. C. and Wirth, A.: Dynamics of turbulent western boundary currents at low latitude in a shallow water model, Ocean Sci. Discuss., 11, 753–788, doi:10.5194/osd-11-753-2014, 2014.

Barnier, B., Reynaud, T., Beckmann, A., Böning, C., Molines, J.-M., Barnard, S., and Jia, Y.: On the seasonal variability and eddies in the North Brazil Current: insights from model intercomparison experiments, Prog. Oceanogr., 48, 195–230, 2001.

Barnier, B., Madec, G., Pendu , T., Molines, J.-M., Treguier, A.-M., Le Sommer, J., Beckmann, A., Biastoch, A., Böning, C., Dengg, J., Derval, C., Durand, E., Gulev, S., Remy, E., Talandier, C., Theetten, S., Maltrud, M., McClean, J., De Cuevas, B.: Impact of partial steps and momentum advection schemes in a global ocean circulation model at eddy-permitting resolution, Ocean Dynam., 56, 543–567, 2006. 739





OSD
12, 735–767, 2015

Beal, L. M. and Donohue, K. A.: The Great Whirl: Observations of its seasonal development and interannual variability, J. Geophys. Res.-Oceans, 118, 1–13, 2013. 736, 737, 744, 752

Beal, L., Hormann, V., Lumpkin, R., and Foltz, G.: The response of the surface circulation of the Arabian Sea to monsoonal forcing, J. Phys. Oceanogr., 43, 2008–2022, 2013. 737, 741

Brodeau, L., Barnier, B., Treguier, A.-M., Penduff, T., and Gulev, S.: An ERA40-based atmospheric forcing for global ocean circulation models, Ocean Modell., 31, 88–104, 2010. 739, 740

Dee, D., Uppala, S., Simmons, A., Berrisford, P., Poli, P., Kobayashi, S., Andrae, U., Balmaseda, M., Balsamo, G., Bauer, P., Bechtold, P., Beljaars, A. C. M., van de Berg, L., Bidlot, J., Bormann, N., Delsol, C., Dragani, R., Fuentes, M., Geer, A. J., Haimberger, L., Healy, S. B., Hersbach, H., Holm, E. V., Isaksen, L., Kallberg, P., Köhler, M., Matricardi, M., McNally, A. P., Monge-Sanz, B. M., Morcrette, J.-J., Park, B.-K., Peubey, C., de Rosnay, P., Tavolato, C., Thépaut, J.-N., and Vitart, F.: The ERA-Interim reanalysis: configuration and performance of the data assimilation system, Q. J. Roy. Meteorol. Soc., 137, 553–597, 2011. 740

Deshayes, J., Tréguier, A.-M., Barnier, B., Lecointre, A., Sommer, J. L., Molines, J.-M., Pendu, T., Bourdallé-Badie, R., Drillet, Y., Garric, G., Benshila, R., Madec, G., Biastoch, A., Böning, C. W., Scheinert, M., Coward, A. C., and Hirschi, J. J.-M.: Oceanic hindcast simulations at high resolution suggest that the Atlantic MOC is bistable, Geophys. Res. Lett., 40, 3069–3073, 2013. 739

DRAKKAR-Group, Barnier, B., Brodeau, L., Le Sommer, J., Molines, J.-M., Penduff, T., Theetten, S., Treguier, A.-M., Madec, G., Biastoch, A., Böning, C., Dengg, J., Gulev, S., Bourdallé-Badie, R., Chanut, J., Garric, G., Alderson, S., Coward, A., de Cuevas, B., New, A. U., Haines, K., Smith, G., Myers, P., Drijfhout, S., Hazeleger, W., and Severijns, C.: Eddy-permitting Ocean Circulation Hindcasts of past decades, Clivar Exchange. Newslett., 12, 8–10, 2007. 739

DRAKKAR Group, Treguier, A.-M., Barnier, B., Blaker, A., Biastoch, A., Böning, C., Coward, A., Deshayes, J., Duchez, A., Hirschi, J., Le Sommer, J., Madec, G., Maze, G., Molines,J-M., New, A., Penduff, T., Scheinert, M., and Talandier, C.: DRAKKAR: developing high resolution ocean components for European Earth system models, Exchanges, Clivar Newslett., No. 65, 19, 2014. 739

Duchez, A., Frajka-Williams, E., Castro, N., Hirschi, J., and Coward, A.: Seasonal to interannual variability in density around the Canary Islands and their influence on the Atlantic meridional overturning circulation at 26° N, J. Geophys. Res.-Oceans, 119, 1843–1860, 2014. 739





OSD

12, 735–767, 2015

Somali Current eddies interactions

C. Q. C. Akuetevi et al.

Evans, R. H. and Brown, O. B.: Propagation of thermal fronts in the Somali Current system, Deep-Sea Res. A., 28, 521–527, 1981. 737, 747
Fischer, J., Schott, F., and Stramma, L.: Currents and transports of the Great Whirl-Socotra Gyre system during the summer monsoon, August 1993, J. Geophys. Res., 101, 3573–3587, 1996. 741, 748
Flament, P.: A state variable for characterizing water masses and their diffusive stability: spiciness, Prog. Oceanogr., 54, 493–501, 2002. 742
Fratantoni, D. M., Bower, A. S., Johns, W. E., and Peters, H.: Somali Current rings in the eastern Gulf of Aden, J. Geophys. Res.-Oceans, 111, C09039, doi:10.1029/2005JC003338, 2006. 741, 752
Jensen, T. G.: Modeling the seasonal undercurrents in the Somali Current system, J. Geophys. Res.-Oceans, 96, 22151–22167, 1991. 737
Johns, W. E., Lee, T. N., Schott, F. A., Zantopp, R. J., and Evans, R. H.: The North Brazil Current retroflection: seasonal structure and eddy variability, J. Geophys. Res.-Oceans, 95, 22103–22120, 1990.
Large, W. and Yeager, S.: The global climatology of an interannually varying air–sea flux data set, Clim. Dynam., 33, 341–364, 2009. 740
Luther, M. E. and O'Brien, J. J.: Modelling the Variability in the Somali Current, Mesoscale/Synoptic Coherent Structures in Geophysical Turbulence, Elsevier, Amsterdam, 373–386, 1989. 738
Madec, G.: NEMO ocean engine, Institut Pierre-Simon Laplace (IPSL), Paris, 2008. 739
Maltrud, M. E. and McClean, J. L.: An eddy resolving global 1/10 ocean simulation, Ocean Modell., 8, 31–54, 2005. 739
Marzocchi, A., Hirschi, J. J.-M., Holliday, N. P., Cunningham, S. A., Blaker, A. T., and Coward, A. C.: The North Atlantic subpolar circulation in an eddy-resolving global ocean model, J. Marine Sys., 142, 126–143, 2015. 739
Maze, G., Deshayes, J., Marshall, J., Tréguier, A.-M., Chronis, A., and Vollmer, L.: Surface vertical PV fluxes and subtropical mode water formation in an eddy-resolving numerical simulation, Deep-Sea Res. Pt. II, 91, 128–138, 2013. 739
Robinson, S. K.: Coherent motions in the turbulent boundary layer, Ann. Rev. Fluid Mech., 23, 601–639, 1991.
Schott, F., Fischer, J., Garternicht, U., and Quadfasel, D.: Summer monsoon response of the northern Somali Current, 1995, Geophys. Res. Lett., 24, 2565–2568, 1997. 738, 748





OSD
12, 735–767, 2015

Somali Current eddies interactions

C. Q. C. Akuetevi et al.

Schott, F. A. and McCreary, J. J. P.: The monsoon circulation of the Indian Ocean, Prog. Oceanogr., 51, 1–123, 2001. 736, 741
Schott, F. A., Xie, S.-P., and McCreary, J. P: Indian Ocean circulation and climate variability, Rev. Geophys., 47, doi:10.1029/2007RG000245, 2009. 736
Sérazin, G., Penduff, T., Grégorio, S., Barnier, B., Molines, J.-M., and Terray, L.: Intrinsic Variability of Sea Level from Global 1/12° Ocean Simulations: Spatio temporal Scales, J. Climate, 28, 4279–4292, doi:10.1175/JCLI-D-14-00554.1, 2015. 740
Swallow, J. C., Molinari, R. L., Bruce, J. G., Brown, O. B., and Evans, R. H.: Development of near-surface flow pattern and water mass distribution in the Somali Basin in response to the southwest monsoon of 1979, J. Phys. Oceanogr., 13, 1398–1415, 1983. 737
Treguier, A. M., Deshayes, J., Le Sommer, J., Lique, C., Madec, G., Penduff, T., Molines, J.-M., Barnier, B., Bourdalle-Badie, R., and Talandier, C.: Meridional transport of salt in the global ocean from an eddy-resolving model, Ocean Sci., 10, 243–255, doi:10.5194/os-10-243-2014, 2014. 739
Valcke, S. and Verron, J.: Interactions of baroclinic isolated vortices: The dominant effect of shielding, J. Phys. Oceanogr., 27, 524–541, 1997. 749
Wirth, A., Willebrand, J., and Schott, F.: Variability of the Great Whirl from observations and models, Deep-Sea Res. Pt. II, 49, 1279–1295, 2002. 737





OSD
12, 735–767, 2015
Somali Current eddies interactions
C. Q. C. Akuetevi et al.

**Table 1.** Specificities of the global model simulations. Only differences between runs are reported. The full model characteristics are described in Drakkar technical reports by Molines (2012) and Lecointre (2012) and are summarized in DRAKKAR group (2014). Model variables are stored every 5 days as 5 day means.

| DRAKKAR Simulation reference | ORCA025.L75-MJM95 | ORCA12.L46-MAL84 | ORCA12.L46-MAL95 |
|---|---|---|---|
| Reference in the paper | MJM95 | MAL84 | MAL95 |
| Horizontal resolution | 1/4° | 1/12° | 1/12° |
| Vertical level (with partial steps) | 75 | 46 | 46 |
| Lateral boundary condition | free slip | free slip | partial slip |
| Initial conditions | From rest, Levitus (1994) | From rest, Levitus (1994) | 10 years spin-up (1978–1988) with CORE forcing |
| Atmospheric forcing | ERAinterim | DFS4.3 | ERAinterim |
| Starting date | 1 January 1989 | 1 January 1978 | 1 January 1989 |
| Ending date | 31 December 2009 | 31 December 1992 | 31 December 2007 |
| Duration | 21 years | 15 years | 30 years |





OSD
12, 735–767, 2015
Somali Current eddies interactions
C. Q. C. Akuetevi et al.

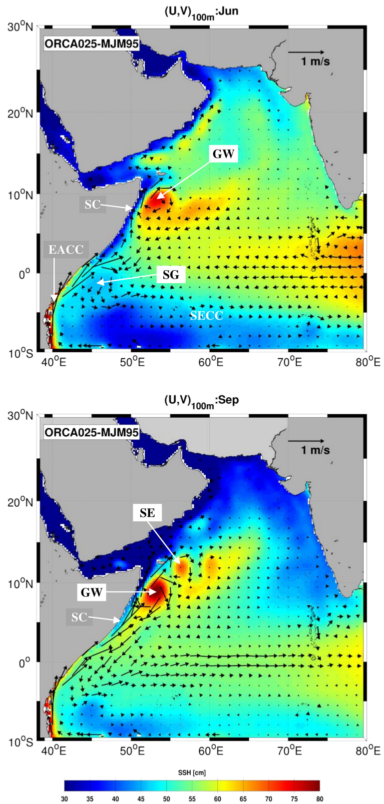


**Figure 1.** June (top) and September (bottom) climatological mean sea surface height (SSH; colour shading; cm) with currents at 100 m depth superimposed (vectors; $m\,s^{-1}$) in the 1/4° MJM95 simulation. The climatological mean is calculated over the last 10 years of the simulation. Landmasses are shaded. SC = Somali Current. EACC=East African Coastal Current. SECC= South Equatorial Counter Current. GW = Great Whirl. SG=Southern Gyre. SE=Socotra Eddy.





OSD
12, 735–767, 2015



Title Page
Abstract | Introduction
Conclusions | References
Tables | Figures
◂◂ | ▸▸
◂ | ▸
Back | Close
Full Screen / Esc
Printer-friendly Version
Interactive Discussion

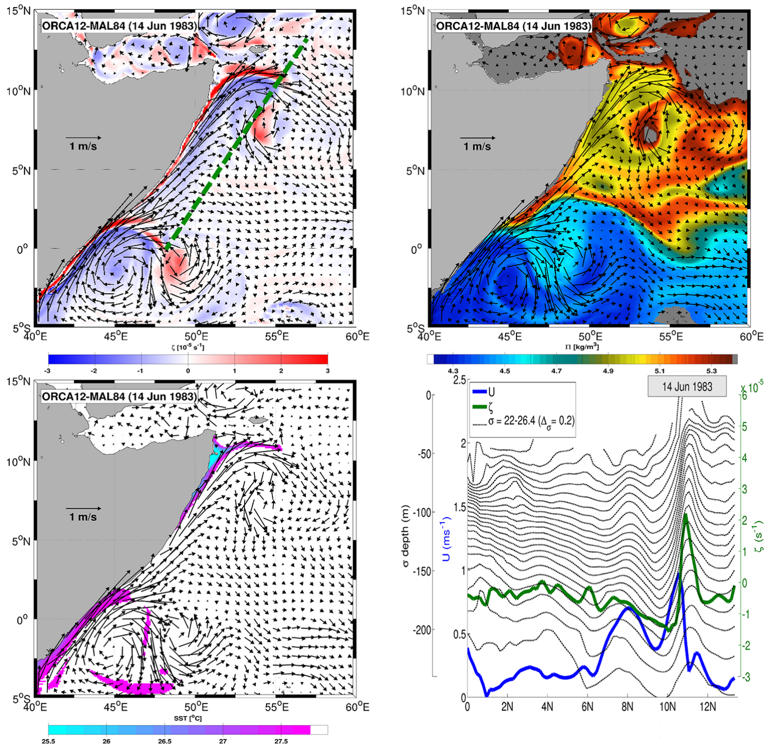


**Figure 2.** Top panels from left to right: snapshot (on 14 June 1984 from the 1/12° MAL84 experiment) of surface currents (vectors; $\mathrm{m\,s^{-1}}$) superimposed on **(a)** the relative vorticity ($\zeta$; color shading; $\mathrm{s^{-1}}$) at depth 50 m, **(b)** the spiciness on $\sigma_0 = 23.8$ ($\Pi$; color shading; $\mathrm{kg\,m^{-3}}$). Bottom panels from left to right: **(c)** the sea surface temperature (SST; color shading; °C), **(d)** the last panel shows along an oblique section parallel to the coast (and passing throughout the Somali eddies as shown on the relative vorticity panel): the depths of the isopycnals comprised in the range $22 \le \sigma_0 \le 26.4$ (black contours by interval of 0.2), the variation of relative vorticity $\zeta$ at 50 m depth (green plot), and the variation of the current speed $U$ at depth 50 m (blue plot).





OSD
12, 735–767, 2015

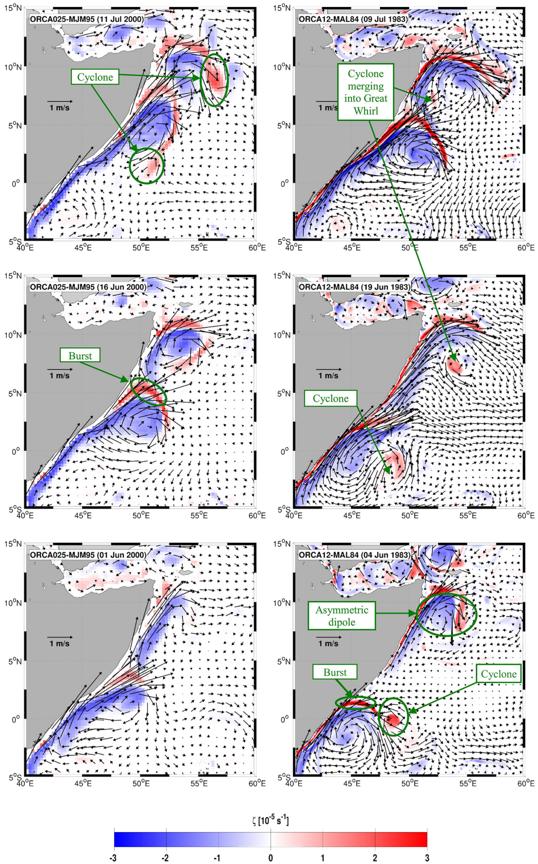


**Figure 3.** Sequence of relative vorticity ($\zeta$; color shading; $s^{-1}$) and currents (vectors; $m\,s^{-1}$) at 50 m depth showing the occurrence of the vorticity bursts and their subsequent development into asymmetric dipoles. The two large pools of negative (blue) vorticity are the SG and the GW. The sequence on the left is from the 1/4° MJM95 simulation and the sequence on the right from the 1/12° MAL84 simulation. Time increases from bottom up.





OSD
12, 735–767, 2015

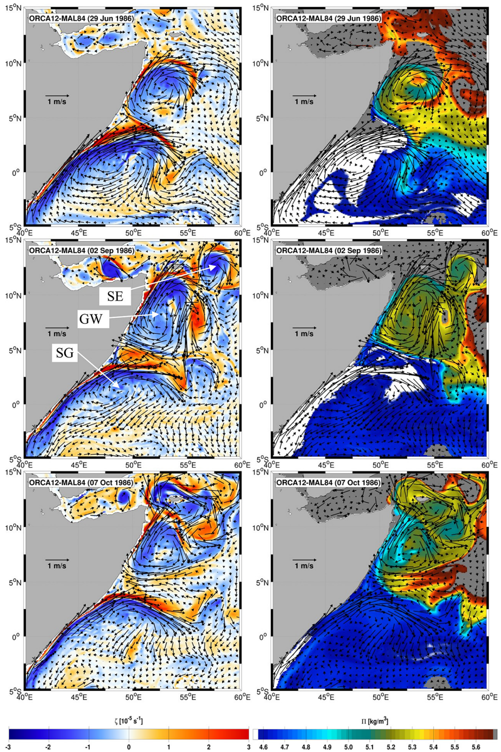


**Figure 4.** Snapshots of current (vectors; $\mathrm{m\,s^{-1}}$) at 50 m superimposed on **(a)** relative vorticity ($\zeta$; color shading; $\mathrm{s^{-1}}$) at 50 m and **(b)** spiciness on isopycnal $\sigma_0 = 23.8$, at 3 different stages of the Southwest Monsoon in 1986 in MAL84 (top: 29 June, middle: 2 September, bottom: 7 October). The Southern Gyre (SG) does not move northward and remains located south of 5° N during the whole monsoon period. The Great Whirl (GW) also remains at its original location. No collision between the SG and the GW occurred this year. A Socotra Eddy (SE) is seen east of the Socotra island.





OSD
12, 735–767, 2015

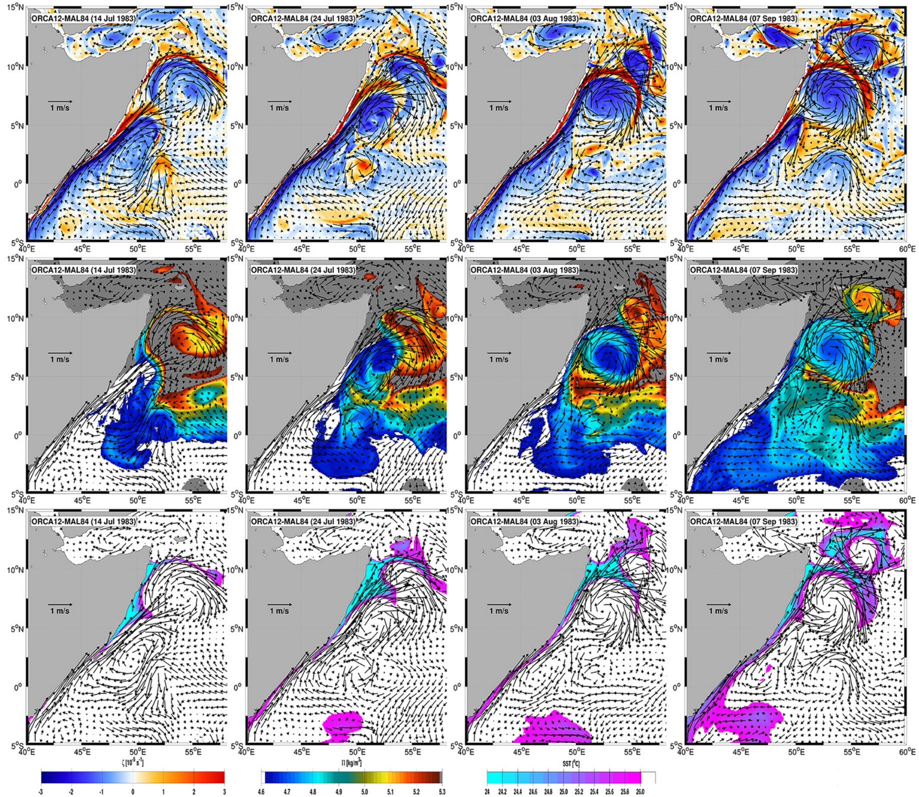


**Figure 5.** Sequence of snapshots describing the most frequent scenario during the well established southwest Monsoon period. Surface currents (vectors; $m\,s^{-1}$) are super imposed on, from left to right; the relative vorticity ($\zeta$; color shading; $s^{-1}$) at depth 50 m, the sea surface temperature (SST, color shading, °C), the spiciness on $\sigma = 23.8$ ($\Pi$; color shading; $kg\,m^{-3}$). This sequence is from the 1/12° MAL84 experiment. It illustrates the collision with no merging between the Great Whirl and the Southern Gyre which leads to the formation of a new Great Whirl and the Socotra Eddy.





OSD
12, 735–767, 2015

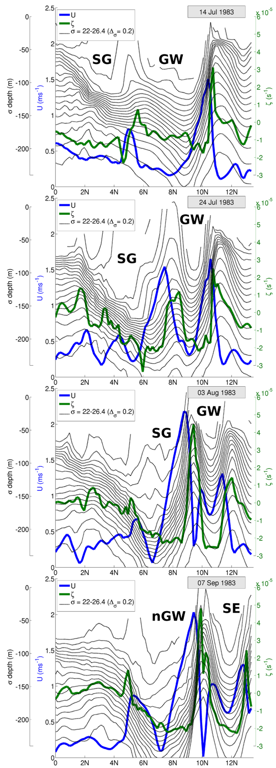


**Figure 6.** Sequence (corresponding to that of Fig. 5) along an oblique section parallel to the coast (and passing throughout the Somali eddies as shown on the relative vorticity panel) of: The depths of the isopycnals comprised in the range $22 \leq \sigma_0 \leq 26.4$ (black contours by interval of 0.2), the variation of relative vorticity $\zeta$ at 50 m depth (green plot), and the variation of the current speed $U$ at depth 50 m (blue plot).





OSD
12, 735–767, 2015

Discussion Paper | Discussion Paper | Discussion Paper | Discussion Paper |

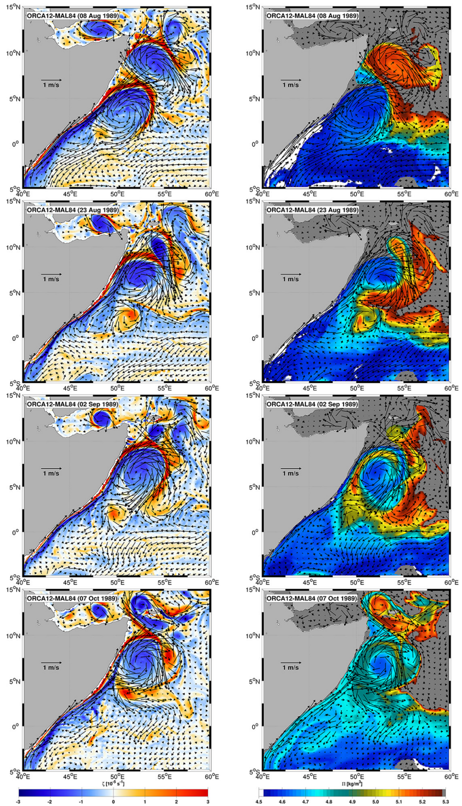

**Figure 7.** Sequence of snapshots describing the rare scenario (2 times over 30 years) during the well-established Southwest Monsoon period. From MAL84 experiment to illustrate the collapse of the two cold wedges and an elastic collision shock between the Great Whirl and Southern Gyre in which the Great Whirl is pushed through the passage of Socotra giving place to the Southern Gyre to become a new Great Whirl.



OSD
12, 735–767, 2015
Somali Current eddies interactions
C. Q. C. Akuetevi et al.

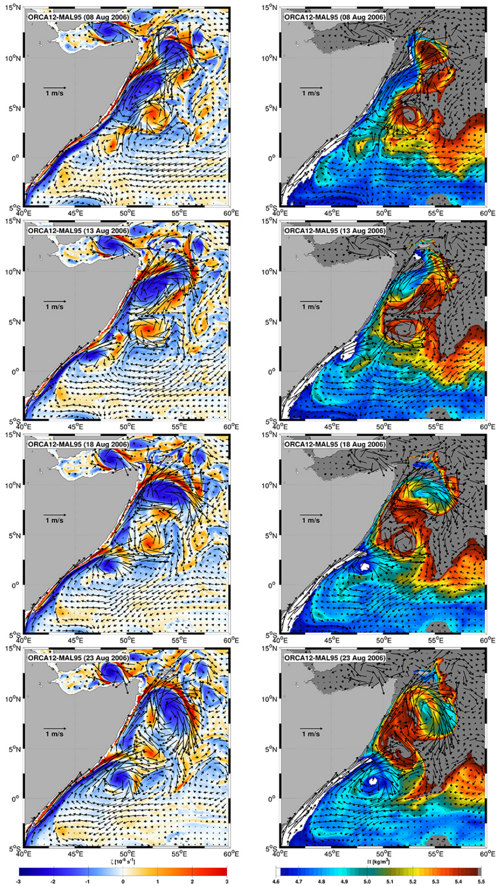


**Figure 8.** Sequence of snapshots describing the unique merging scenario from MAL95 experiment.



OSD

12, 735–767, 2015

Somali Current eddies interactions

C. Q. C. Akuetevi et al.

Title Page
Abstract Introduction
Conclusions References
Tables Figures
◀ ▶
Back Close
Full Screen / Esc
Printer-friendly Version
Interactive Discussion

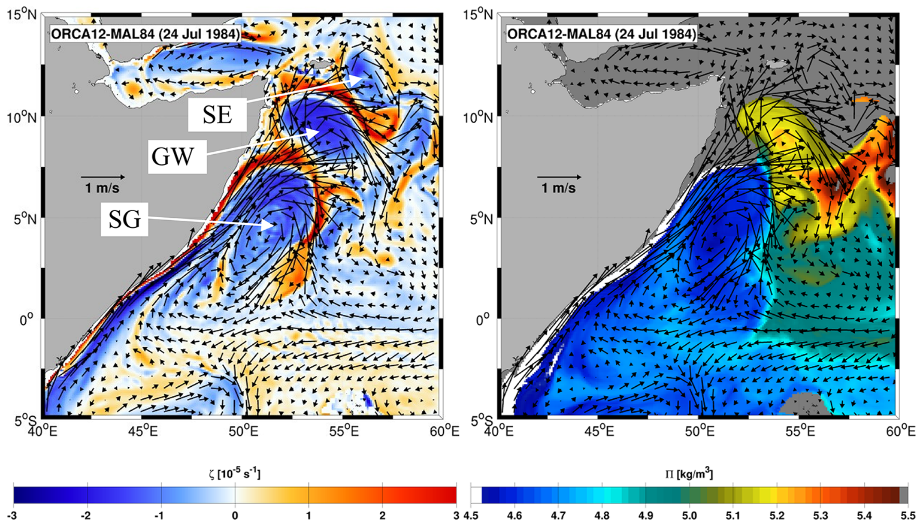


**Figure 9.** Snapshot on 24 July 1984 of the current (vectors; $\mathrm{m\,s^{-1}}$) at 50 m depth superimposed on **(a)** relative vorticity ($\zeta$; color shading; $\mathrm{s^{-1}}$) at 50 m depth and **(b)** spiciness on isopycnal $\sigma_0 = 23.8$ in the 1/12° MAL84 experiment. SE = Socotra Eddy, GW = Great Whirl, and SG = Southern Gyre.